Nano Biomed Eng
2017, 9(4): 314-323. doi: 10.5101/nbe.v9i4.p314-323.

Research Article

An in-vitro Cytotoxic and Genotoxic Properties of *Allamanda Cathartica L.* Latex Green NPs on Human Peripheral Blood Mononuclear Cells

Prabhu Das Nelaturi[1], Nandhini Huthur Sriramaia[1], Sudeep Nagaraj[1], Venkata Subbaiah Kotakadi[2], Ambalath Veetil Veeran Moideen Kutty[1], Kiranmayee Pamidimukkala[1]

[1]Department of Cell Biology and Molecular Genetics, Sri Devaraj Urs Academy of Higher Education and Research, Tamaka, Kolar-563 103, Karnataka, India.
[2]DST-PURSE Centre, Sri Venkateswara University, Tirupati-517502, Andhra Pradesh, India

Corresponding author. E-mail: kiranmayee@sduu.ac.in

Received: Nov. 22, 2017; **Accepted:** Dec. 24, 2017; **Published:** Dec. 27, 2017.

Citation: Prabhu Das Nelaturi, Nandhini Huthur Sriramaiah, Sudeep Nagaraj, Venkata Subbaiah Kotakadi, Ambalath Veetil Veeran Moideen Kutty, and Kiranmayee Pamidimukkala, An in-vitro Cytotoxic and Genotoxic Properties of *Allamanda Cathartica L.* Latex Green NPs on Human PBMCs. *Nano Biomed. Eng.*, 2017, 9(4): 314-323.
DOI: 10.5101/nbe.v9i4.p314-323.

Abstract

Green synthesis of silver nanoparticles (NPs) by green route approaches has advantages over conventional methods. In green synthesis, we use eco-friendly plant extracts contain secondary metabolites and bioactive components, proteins that act as both reducing and capping agents, form stable and shape-controlled green silver nanoparticles. The current study deals with the synthesis of silver nanoparticles using the aqueous latex extract of *Allamanda cathartica*. The green silver nanoparticles are characterized by using different spectroscopic methods like ultra violet-visible spectroscopy (UV-Vis), Fourier transform-infrared spectroscopy (FTIR), transmission electron microscope (TEM), scanning electron microscope (SEM) and X-ray diffraction (XRD). Results indicated that the crystalline natured particles were spherical shaped with an average of 35 nm in size, and that the stability of silver nanoparticles was due to its high negative zeta potential of –27.6 mV. The current study also revealed that green silver nanoparticles had very good genotoxic and cytotoxic activity in peripheral blood mononuclear cells (PBMCs). Leukemia leads to the development of high numbers of white blood cells, which is one of the major types of cancers that affect children. Many of the chemicals used for the treatment produce remarkable side effects. To overcome this problem, we made an attempt to see the efficacy of latex green silver nanoparticle on peripheral blood mononuclear cells and deoxyribonucleic acid fragmentation, which leads to the development of future therapeutic drugs.

Keywords: Genotoxic and cytotoxic studies; Green Ag NPs; Human PBMCs; Spectral analysis; SEM; TEM; Zeta potential

Introduction

The basic concept of nanotechnology is the engineering of functional systems at the molecular scale. Nanoparticle (NP), a most popular term and the field of nanotechnology, is one the most active research area. NPs are the essential measure of nanotechnology. The most noteworthy attribute of NPs is that they exhibit large surface area to volume ratio [1]. In general, particles with a size less than 100

nm are referred to as NPs. Metal NPs have gained importance because of their unique physicochemical characteristics, including catalytic, optical, electronic, magnetic properties and antimicrobial activities [2, 3]. Many processes are currently available for synthesizing metal NPs. There is an obvious necessity for an alternative, cost-effective ecofriendly method for NP production, since these productions are expensive, labor intensive and bio-hazardous [4]. Due to their withstanding ability to harsh process conditions, inorganic metal oxides have been paid much attention to by researchers [5]. Silver is one of the important members of the metals used for synthesizing NPs, and many plant extracts have shown to be useful in biosynthesis of silver NPs [6, 12, 13].

Plants have proven to be one of the richest sources of natural products, most of which are therapeutically useful. Plant extracts reduce the metal ions in a shorter time as compared to any other source. When compared to others, NPs synthesized from plants takes a few minutes to hours, depending on the plant type and the concentration of phytochemicals [14]. Several factors together are responsible for the formation of NPs such as plant source pigments, alkaloids, polyphenols and proteins present in the plant extract [15]. Several reports suggested that the phytochemicals, that is, pectins, flavonoids, terpenoids, ascorbic acid, sugars, carotenoids and myriad present in plant materials act as reducing agents as well as a capping agent in the conversion of metal ions to form stable NPs [16]. Of about 10% of flowering plants of Angiosperms contain milky fluid called latex [17]. Latex contains alkaloids, resins, proteins, starches, sugars, oils, tannins, and gums that coagulate on exposure to air. It is usually exuded after tissue injury. In most plants, latex is white, but some have yellow, orange or scarlet latex [18].

Allamanda belongs to Apocynaceae. This plant is well known in traditional medicine to treat various ailments. The whole plant, including leaves, roots and flowers, contains cathartic. Some species of *Allamanda* are active against carcinoma cells, the human immunodeficiency virus (HIV) and pathogenic organisms [19]. Keeping in view the medicinal properties of latex from *Allamanda* and by using green technology in the present study, we tried synthesizing and characterizing green NPs. We characterized green Ag NPs, and the synthesized particles were tested against human peripheral blood mononuclear cells (PBMCs) to find out their antiproliferative activity. Leukemia leads to the development of high numbers of white blood cells [20]. It is one of the major types of cancers that effect children. Many of the chemicals used for the treatment produce remarkable side effects. To overcome this problem, we made an attempt to see the efficacy of latex silver NPs on PBMCs and DNA fragmentation. The overall process of the present study was represented in schematic diagram as given below (Schematic 1).

Schematic 1 Green synthesis of silver NPs by using 3% latex of *Allmanda cathartica* and its spectral characterization and cytotoxic studies on PBMCs.

Experimental

Biosynthesis of NPs

Chemicals: Silver nitrate ($AgNO_3$), sodium dodecyl sulfate (SDS), Tris-EDTA (TE), phosphate buffer solution (PBS), FicollHisep™ leukocyte separation medium (LSM), Roswell Park Memorial Institute (RPMI) 1640 medium, fetal bovine serum (FBS), antibiotics (penicillin, streptomycin, amphotericin), phytohemagglutinine (PHA), dimethyl sulfoxide (DMSO), heparin vacutainer, trypan blue dye, agarose, proteinase K, RNase, and DNA loading dye.

All the aqueous solutions and buffers were prepared by distilled water wherever necessary.

Plant material: The plant material, *Allmanda cathartica* was identified in the garden of Sri Devaraj Urs Medical College, Kolar. During flowering, the plant material was authenticated by Horticulture College, Kolar. Actively growing younger twigs were collected in morning hours at the time of pruning. Milky white latex was collected from these twigs and stored at 4 ℃.

Synthesis of green NPs

For the synthesis of metal NPs, 3% aqueous latex solution was made with distilled water and stored at –20 °C till further use [20]. To 20 mL of 1 mM silver nitrate solution, equal volumes of 3% latex solution were mixed thoroughly and incubated at 37 ℃ for 24 h at 135 rpm in the shaker cum incubator. After incubation, development of reddish brown color was observed and therefore indicated the formation of green silver NPs. These particles were stored in 4 ℃ till further analysis.

Characterization of NPs

Ultraviolet-visible (UV-visible) spectrophotometer allows identification, characterization and analysis of metallic NPs. UV-visible absorption spectra were obtained from Nanodrop 8000, (UV-visible spectrometer, Thermo Scientific) in 200-700 nm wavelength range. Scanning and transmission electron microscopy (SEM and TEM) methods are common for surface and morphological characterization at nanometer to micrometer scale. SEM and TEM were carried out at Department of Microbiology and Cell Biology (MCBL), Indian Institute of Science, Bangalore. Sample preparation for SEM was carried out according to Banerjee et al. [18, 21] with a little modification. Briefly, about 2 mL of the green NP solution was centrifuged at 4000 rpm for 20 min. The pellet was dried and used for SEM. The pellet was scrapped carefully with a forceps and transferred onto a clean glass slide; the images were obtained in a scanning electron microscope, Quanta 200 (FEI). TEM analysis was carried out with carbon coated copper 300 mesh grids. The sample was prepared by placing 10 µL of green silver NP solution on metal-coated copper grids and dried under lamp. The images were obtained from Tecnai G2 Spirit BioTWIN at a voltage of 120 kV. The X-ray diffraction (XRD) pattern measurements of drop-coated films Ag NPs on aluminum foil substrate were recorded in a wide range of Bragg angle 2θ at a scanning rate of 2/min, and carried out on a spectroscope by using Seifert Rayflex 300TT X-ray diffractometer with CuK (λ = 1.542 Å) radiation that was operated at a voltage of 40 kV and a current of 30 mA with Cu k-α radiation (1.5405 Å). Particle size and zeta potential measurement experiments were carried out by using a Nanopartica (HORIBA Instrument). Fourier transform infrared spectroscopy (FTIR) is useful to reveal the organic functional groups that are attached to the surface of NPs. FTIR of the particles was carried out in Spectroscopy Analytical Test Facility, Society for Innovation and Development (SID), Indian Institute of Science, Bangalore with Nicolet 6700 FTIR. The scan range was 4000/cm to 400/cm by potassium bromide (KBr) pellet method.

Collection of peripheral blood and isolation of lymphocytes

The PBMCs were isolated from the left over blood collected in heparin vacutainers from the Central Diagnostic Laboratory of Sri Devaraj Urs Medical College, after getting ethics clearance (SDUAHER/KRL/Res. Project/128/2017-‘18) from the institute. To about 1 mL of the blood was added equal volume of cold PBS (pH 7.0), which was mixed properly and carefully layered onto 2 mL Ficol in a falcon tube without getting mixed up. The contents were spun down at 3000 rpm for 30-45 min at room temperature. Without disturbing the buffy coat layer, plasma was removed, and then the buffy coat was aspirated. The buffy coat was washed with PBS. The growth medium was prepared by mixing RPMI medium, FBS and anitbiotic/antimycotic. The details of the samples and controls are given in Table 1. About 1 mL of RPMI medium was dispensed into falcon tubes, and into it were added 30 µL of PHA and 100 µL of PBMCs. The number of cells was counted in 10 µL and incubated with an atmosphere of 95% air and 5% CO_2 at 37 ℃ for 4 h [19, 22].

Table 1 The number of controls and treatments made in the present study

Control	Only PBMCs PBMCs + DMSO (20 µl) PBMCs + DMSO (100 µL) PBMCs + 1 mM metal solution (20 µL) PBMCs + 1 mM metal solution (100 µL) PBMCs + 3% latex (20 µL) PBMCs + 3% latex (100 µL)
Treatment (concentration)	Green NPs at 20 µg/mL concentration Green NPs at 40 µg/mL concentration Green NPs at 60 µg/mL concentration Green NPs at 80 µg/mL concentration Green NPs at 100 µg/mL concentration

Treatment of lymphocytes with green NPs

After 4 h of incubation, the lymphocytes were inoculated with 20, 40, 60, 80 and 100 µg/mL of the green NPs from 1 mg/mL stock. Lymphocytes in culture media without particles were considered as controls. All the treatments were performed in triplicate, and the mean (± standard error) was calculated in each case. The tubes were kept in a CO_2 incubator at 37 °C for 72 h and monitored regularly.

Trypan blue dye exclusion method

Trypan blue dye exclusion is a cell viability assay based on the ability of the live cells to exclude the vital dye, trypan blue [20, 23]. Equal volumes of cell suspension and trypan blue (0.4% trypan blue in balanced salt solution) were mixed and left for 10 min at room temperature. For viability, about 10 µL trypan blue treated cell solution was counted onto the haemocytometer and observed under microscope. Percentage viability was calculated by applying the following formula:

$$\text{Percent viability} = \frac{\text{Number of viable cells}}{\text{Total number of cells}} \times 100$$

DNA fragmentation assay

About 10^4 cells were taken further for DNA fragmentation assay. DNA fragmentation assay was done with Tris-EDTA and SDS (TES) lysis buffer [24]. Solutions were prepared as mentioned in the protocol viz. 1 M Tris, 20 mM EDTA and 1% SDS. Aliquoted 200 µL of lymphocytes were centrifuged at 2000 rpm for 5 min, and then the supernatant was discarded. To the pellet, 20 µL of TES buffer was added to lyse the cells by mixing properly. To this, 10 µL of RNase was added and was incubated for 1 h at 37 °C. After incubation, 10 µL of proteinase K was added and incubated at 50 °C for 1.5 h. The entire volume was loaded in 1% agarose gel using 6 × blue DNA loading dye and ran the gel at 80-100 V. After the run, the gel image was taken by using UV-trans illuminator and the image was documented.

Statistical analysis

All the experiments were conducted in triplicates and standard errors were calculated wherever needed.

Results and Discussion

In the present study, silver NPs were synthesized by using aqueous extract of *Allamanda cathartica* latex. When 3% latex was mixed with 1 mM silver nitrate solution, within 20 min, the solution turned pale yellow. This was in agreement with *Allamanda* leaf extract [7, 8, 11, 25], and upon overnight incubation there developed clear reddish brown, indicating the formation of silver NPs due to the conversion of Ag^+ ions to elemental Ag by extracellular latex (Fig. 1) on account of the surface plasmon resonance (SPR) phenomenon. During the process of reduction, the silver nitrate solution was reduced to silver ions (Ag^+), i.e. silver NPs (Ag NPs) with the help of phyto-constituents present in the extracellular latex extract of *Allmanda cathartica*. The color change from pale coloration of the solution to dark color was read in UV-visible spectrophotometer for further confirmation.

UV-visible spectrophotometry (UV-Vis)

The UV-visible spectra (Fig. 2) of the reaction solution showed an absorbance peak at 455 nm, which is characteristic SPR peak of Ag NPs, and hence confirmed their synthesis.

Fig. 1 Biosynthesized green NPs after incubation of 3% latex extract with 1 mM $AgNO_3$ presented a change in colour, indicating the development of NPs.

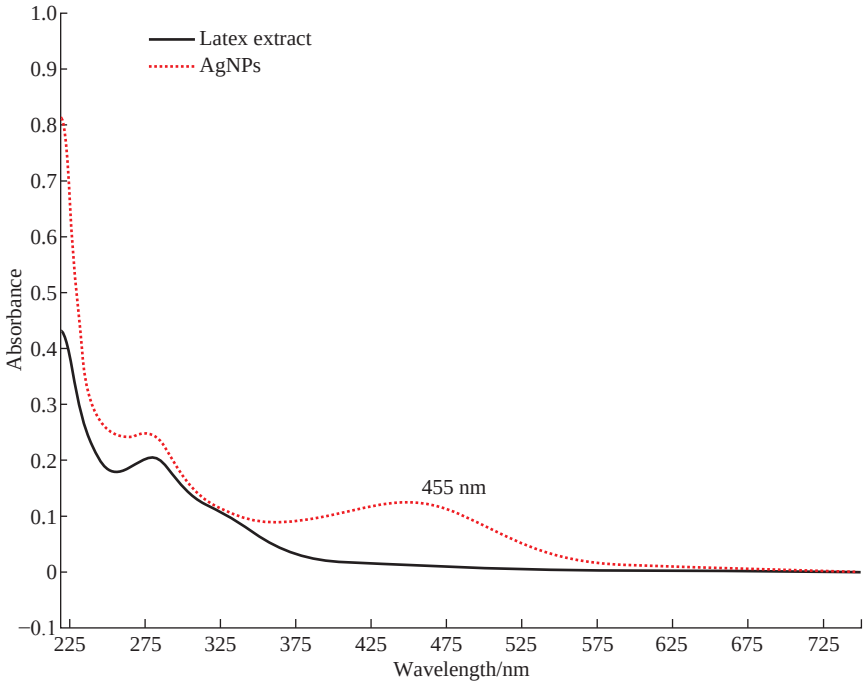

Fig. 2 UV-visible spectra of $AgNO_3$ particles with 3% latex.

This strong absorption peak in the visible range was due to surface plasmon vibrations excited. It is known that the size and shape of NPs reflect the absorbance peak. In fact, the size has a linear correlation with the peak intensity, while the number of NPs does not have such linear correlation [26]. SPR peak could correspond to the spherical shape of metal NPs. This SPR peak was due to the different metabolites and proteins present in the aqueous extract. UV-visible spectroscopy of Ag NPs showed maximum absorption at critical wavelength, corresponding to the absorption maxima of Ag NPs, i.e., at 455 nm. This was in agreement with Harekrishna et al. [20] and other reported results [10, 11]. Further FTIR analysis was carried out to confirm which functional groups had participated in the reduction of green silver NPs.

Fourier transforms infrared spectroscopy (FTIR) analysis

FTIR detected inorganic and organic functional groups of the particles. The FTIR spectrum of latex green NPs is presented in Fig. 3.

The peak at 3150.98 indicates O—H; the peak at 2922.65 is C—H; the peak at 2849.40 is C—H; the peak at 2351.91 is C═C; the peak at 1730.13 indicates either C—C or C—O or C—N; and the peak at 1402.33 indicates C—N or C—O or C—C. The FTIR spectrum of silver NPs from the above figure reveals that the hydroxyl group with the stretch of (O—H, 3150.98; C—H, 2922.65, 2849.40) and the carbonyl group with the stretch of alkenes groups (C ═ C, 2351.91; C═O, 1730.13/cm; C—N 1402.33) were involved in the reduction of Ag^+ to Ag. A similar type of results was also presented in the research by Litvin and Minaev [27, 28]. Therefore, it may be concluded that the water soluble essentials secondary metabolites are responsible for capping and efficient stabilization [8, 22].

Morphology of green silver NPs with transmission electron microscopy (TEM)

TEM provides the images of a sample by scanning it with a focused beam of electrons. When there is an interaction between electrons of the metal and electrons of the sample, various signals can be detected and they contain the information about the sample's surface topography and composition. TEM provides the morphology, i.e., the shape and size details of the particles. From the instrument, thirteen particles were captured, and by using ImageJ software, the area, angle, length and diameter of the particles were measured (Table 2, Fig. 4 and 5).

The average diameter of the particles was 34.69 nm. The shape of the particles was spherical, rectangular, round and angular. TEM images showed that the particle size ranged from 19-52 nm. The particles are spherical, rectangular, a few with striations, uniformly distributed without any aggregation [9].

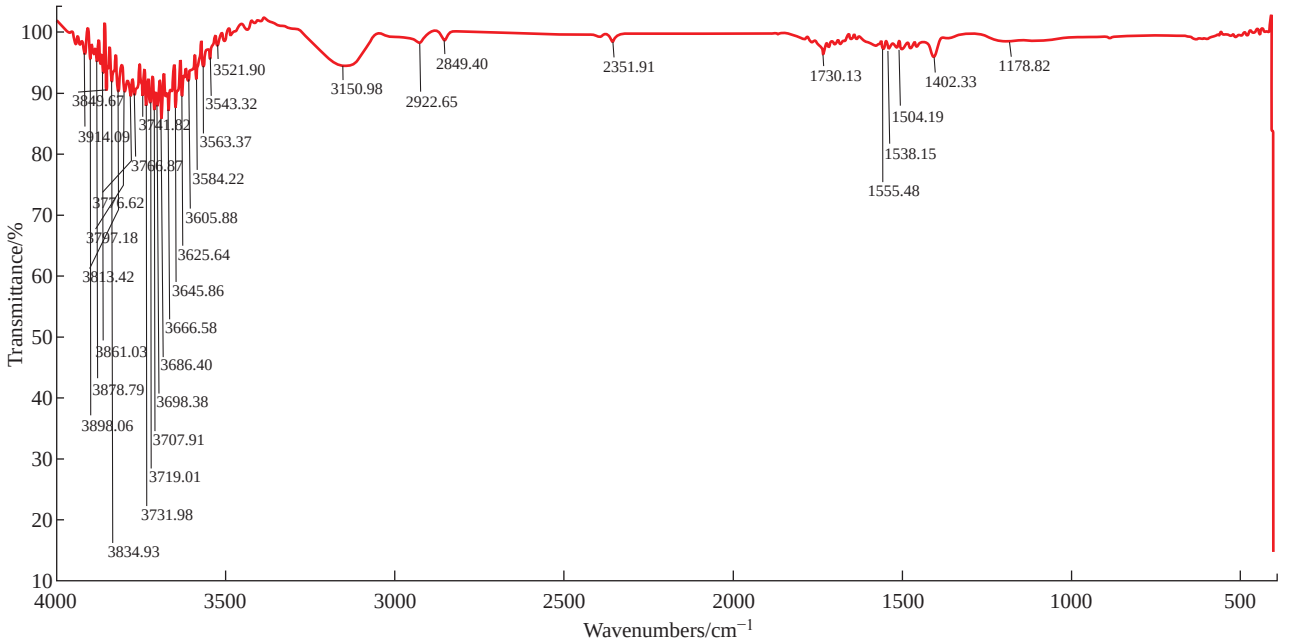

Fig. 3 FTIR analysis of biosynthesized green NPs.

Table 2 Measurement of green NPs from ImageJ software

S. No.	Area	Mean	Min	Max	Angle	Length	Diameter
1.	4.43	59.664	0.195	228	5.711	44.219	
	1575.92	69.495	0	254	5.711	44.219	44.79
2.	5.76	44.803	4.306	135	138.664	57.535	
	1614.23	50.133	0	254	0	0	45.33
3.	4.22	37.403	2.687	106.883	161.737	42.122	
	782.53	50.216	0	254	0	0	31.56
4.	3.24	16.838	0	110	68.199	32.311	
	327.95	20.062	0	144	0	0	20.43
5.	3.52	18.2	0	127	133.152	35.091	
	1037.24	38.489	0	254	0	0	36.34
6.	2.52	33.295	2.695	116	141.483	25.05	
	501.44	52.555	0	254	0	0	25.26
7.	4.6	30.064	0	163.392	132.879	45.852	
	1760.53	65.657	0	254	0	0	47.34
8.	2.53	17.759	0	92	14.697	25.225	
	309.1	28.653	0	222	0	0	19.83
9.	6.16	64.935	27.598	212.884	18.199	61.475	
	1387.77	68.378	4	254	0	0	42.03
10.	3.27	23.058	0	76.293	19.323	32.639	
	733.96	34.215	0	212	0	0	30.56
11.	2.98	70.798	37.482	140.132	19.654	29.732	
	643.35	80.111	24	222	0	0	28.62
12.	6.27	35.548	27.8	136	97.716	62.566	
	2196.72	41.784	0	226	0	0	52.88
13.	2.53	21.078	0	120.048	17.571	25.175	
	528.76	36.871	0	249	0	0	25.94

Scanning electron microscopy (SEM) analysis

Morphology of synthesized NPs was characterized by SEM analysis. Fig. 6 shows the SEM images obtained upon equal volumes of 3% latex and 1 mM silver nitrate solution. SEM revealed that the NPs were mostly spherical, polydisperse, and not in direct contact with each other even within the aggregate. This indicated that the synthesized NPs were stabilized

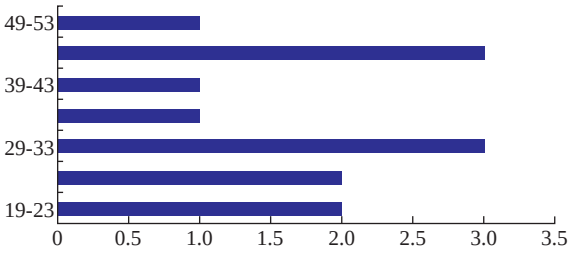

Fig. 4 Particle size distribution histogram of silver NPs determined from TEM image. The minimum and maximum diameters of the particles were 19.83 nm and 52.88 mn.

by a capping agent (Fig. 5). The similar result has been observed with silver NPs synthesized with plant extracts [7, 9] and fungal extract [29].

XRD analysis

The crystalline nature of the green synthesized Ag NPs by latex of Allamanda was also confirmed by XRD pattern analysis. The XRD pattern in Fig. 6 indicated that the particles had a face-centered cubic structure. There were three distinct reflections in the

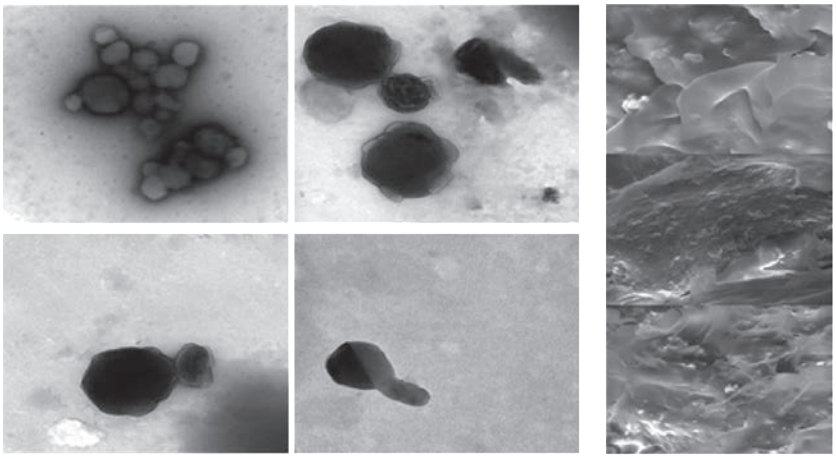

Fig. 5 (a) TEM; and **(b)** SEM images of Ag NPs.

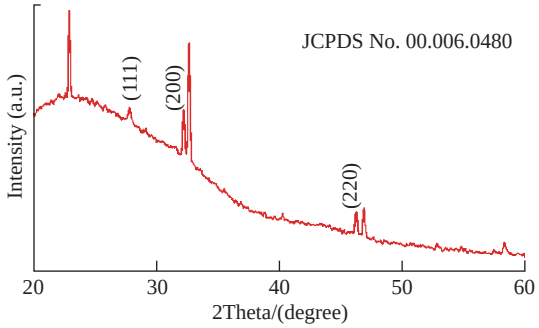

Fig. 6 XRD analysis of silver NPs.

diffractogram at 27.83° (111), 32.24° (200) and 46.23° (220) (JCPDS Card No. 06-0480). The absence of any additional reflections other than the reflections belonging to the Ag lattice clearly suggested that the green synthesized Ag NP lattice was unaffected by other molecules in the plant extract.

Particle size determination

Particle size of the biosynthesized green Ag NPs was determined by laser diffraction intensity which revealed that the particles obtained were polydisperse in nature with particle size ranging from 22.2 to 35 nm (Fig. 7). The Z-average diameter of the particles was found to be 41.1 nm. The results were similar to the results obtained in TEM analysis.

Zeta potential measurement

The zeta potential of the synthesized Ag NPs was found to be –27.6 mV (Fig. 8) in water as dispersant. On the other hand, the electrostatic repulsive forces between the NPs when they were negatively charged possibly protected them from forming an association. This prevented the particles from agglomeration in the medium, leading to long term stability.

The high value of zeta potential confirmed the repulsion among the particles which thereby increased the stability of Ag NPs and their formulation [8]. The Ag NPs in the present study were negatively charged with a zeta potential of –27.6 mV, which proved evident that the particles were dispersed in the medium.

Cytotoxicity of particles on PBMCs

The PBMCs were treated with 20, 40, 60, 80 and 100 µg/mL of green synthesized NPs from 1 mg/mL

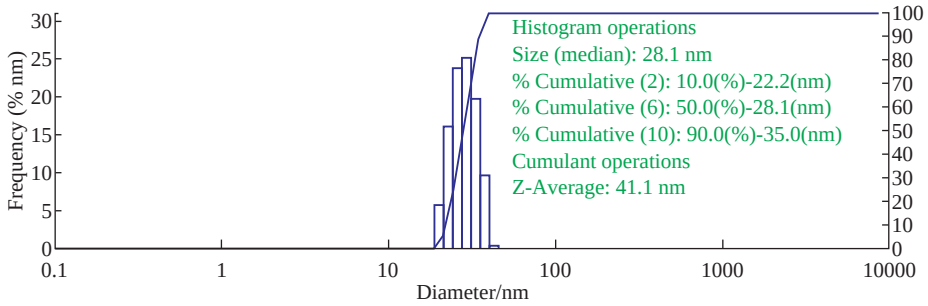

Fig. 7 Particle size/Dynamic light scattering (DLS) analysis of silver NPs.

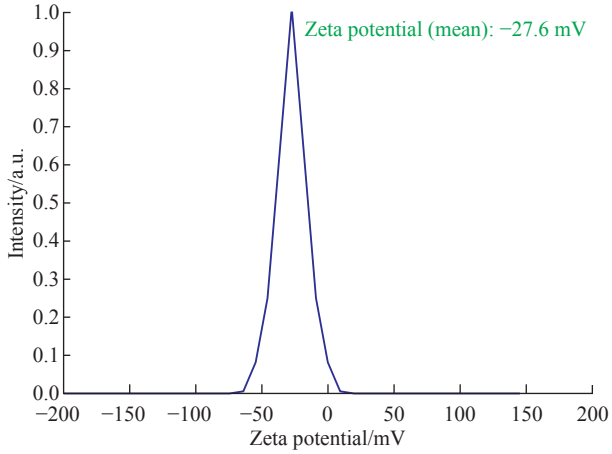

Fig. 8 Zeta potential analysis of silver NPs.

stock. After 72 h, trypan blue dye exclusion method was used to reveal the percentage cell viability of both control and treated cells. The results showed dose dependent response. As the concentration of green NPs increased, the percentage of dead cells increased and the percentage of live cells decreased. In the control wherein only PBMCs were present, the percentage viable cells and percentage non-viable were noted as 67 and 33%. In other controls, only minimum and maximum concentrations were taken into consideration. With the control of PBMCs with DMSO, 100 µL showed higher dead cell percentage (71%) than 20 µL (33%). With $AgNO_3$ metal solution at 1 mM concentration, both 20 and 100 µL showed almost the same percentage of viable and non-viable cells, i.e., 71 and 75%. Similar to the metal control, PBMCs with 3% latex showed similar percentage viability and non-viability for 20 and 100 µL as of 39% and 36% respectively (Table 3, Fig. 9).

These results demonstrated the Ag NPs mediated concentration-dependent toxicity on PBMCs. This provides a basis for understanding the toxicity of latex

Table 3 Percentage of viable and non-viable cells when PBMCs were treated with different concentrations of green NPs. Values are expressed as mean ± S.E.

S. No.	Sample	No. of cells		Total cells	% Viable cells	% non-viable cells
		Live	Dead			
1.	Control	127	62	189	67 ± 0.57	33 ± 0.57
2.	PBMCs + DMSO (20 µl)	62	31	93	67 ± 1.1	33 ± 2.3
3.	PBMCs + DMSO (100 µl)	22	55	77	29 ± 0.57	71 ± 0.57
4.	PBMCs + 1 mM metal solution (20 µL)	12	29	41	29 ± 1.1	71 ± 2.3
5.	PBMCs + 1 mM metal solution (100 µL)	17	51	68	25 ± 1.1	75 ± 1.7
6.	PBMCs + 3% latex (20 µL)	46	30	76	61 ± 0.57	39 ± 0.57
7.	PBMCs + 3% latex (100 µL)	58	33	91	64 ± 1.1	36 ± 1.1
8.	Green NPs at 20 µg/mL concentration	25	14	39	64 ± 1.1	36 ± 1.1
9.	Green NPs at 40 µg/mL concentration	13	14	27	48 ± 1.1	52 ± 1.7
10.	Green NPs at 60 µg/mL concentration	22	24	46	48 ± 1.1	52 ± 0.5
11.	Green NPs at 80 µg/mL concentration	26	36	62	42 ± 0.5	58 ± 0.57
12.	Green NPs at 100 µg/mL concentration	10	38	48	21 ± 1.1	79 ± 1.1

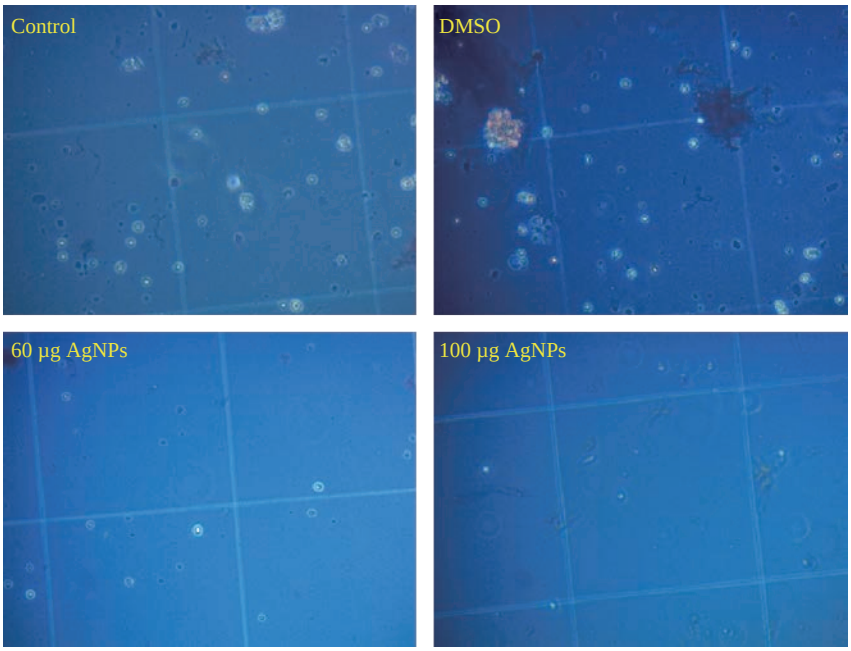

Fig. 9 Trypan blue images of cells when treated with DMSO, silver nitrate, latex and different concentrations of green Ag NPs.

NPs and cellular uptake [30]. Several studies explained that the Ag NPs disrupted normal cellular functions, influencing the membrane integrity and inducing programmed cell death [31].

DNA fragmentation assay

We examined the influence of Ag NPs on DNA fragmentation. The induction of DNA fragmentation is a predicted marker for DNA damage of PBMCs. In the present study, NPs showed apoptotic fragmentation of lymphocyte DNA (Fig. 10).

This might be due to interaction between silver atoms and the functional groups of proteins and DNA. DNA fragmentation assay indicates the extraction of DNA from lysed cells which is followed by Agarose gel electrophoresis. We examined the effect of silver NPs on DNA fragmentation. The gel electrophoresis revealed that the intensity of DNA was diminished because of the cleavage of DNA so fragments of DNA were noted. The NPs produce oxidative stress which causes DNA damage. Excessive production of ROS,is known to induce apoptosis [32].

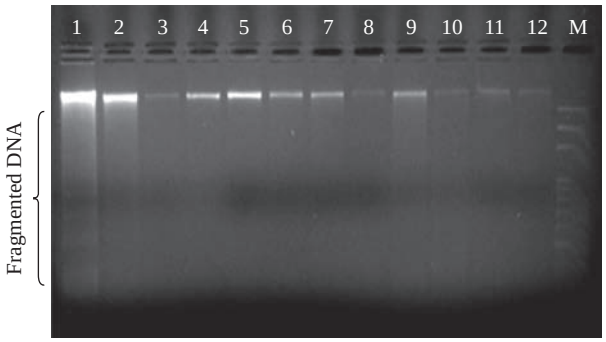

Fig. 10 Agarose gel electrophoresis of PBMC DNA: (1) Control 1; (2) & (3) DMSO; (4) & (5) Latex; (6) & (7) Silver nitrate; (8)-(12) Different concentrations of green Ag NPs; and (13) DNA ladder.

Conclusions

Allmanda cathartica latex extract was found to be suitable for quick synthesis of green Ag NPs by green synthesis within 20 min to overnight. Spectral analysis of green Ag NPs by UV-Vis, FTIR, SEM, TEM, particle size and zeta potential support the formation and stability of the bio-synthesized green Ag NPs. The average size of green silver NPs was found to be 35 nm. Hence, the current study also reveals that green Ag NPs have very good genotoxicity and cytotoxicity activity in PBMC. As leukemia leads to development of high numbers of white blood cells, *to overcome this problem, we made an attempt to see the efficacy of latex green silver NPs on PBMCs and DNA fragmentation,* which leads to the development of future therapeutic drugs.

Acknowledgements

Authors are grateful to the Department of Cell Biology and Human Genetics, Sri Devaraj Urs Academy of Higher Education and Research for providing the facilities to carry out this work.

Conflict of Interest

The authors declare that no competing interest exists.

References

[1] A. Leela, M. Vivekanandan, Tapping the unexploited plant resources for the synthesis of silver NPs. *African J of Biotech*, 2008, 7(17): 3162-3165.

[2] S.V. Bharathi, A, Ahmad, and S.M. Tajo, Silver NP synthesis using C. caesia and C. amada rhizome extract. *Inter J of Pharm Tech Res*, 2015, 8(7): 142-145.

[3] M. Murugan, K.K. Shanmugasundaram, Biosynthesis and characterization of silver NPs using the aqueous of Vitex negundo Linn. *World J of Pharmacy and PharmaSci*, 2014, 3(8): 1385-1393.

[4] P. Raveendran, J. Fu, and S.L. Wallen, Completely "green" synthesis and stabilization of metal NPs. *J of the American Chem Society*, 2003, 125: 13940-13941.

[5] W. Yu, H. Xie, A review on nanofluids: preparation, stability mechanisms, and applications. *J of Nanomaterials*, 2012, 2012: 435873.

[6] K. Logaranjan, S. Devi, and K. Pandian, Biogenic synthesis of silver NPs using fruit extract of Ficus carica and study its antimicrobial activity. *Nano Biomed Eng*, 2012, 4(4), 177-182.

[7] V.S. Kotakadi, Y. SubbaRao, S.A. Gaddam, et al., Simple and rapid biosynthesis of stable silver NPs using dried leaves of Catharanthusroseus. Linn. G. Donn and its antimicrobial activity. *Colloids and Surf. B: Biointerfaces*, 2013, 105: 194-198.

[8] V.S. Kotakadi, S.A. Gaddam, S.K. Venkata, et al., Ficus fruit-mediated biosynthesis of silver NPs and their antibacterial activity against antibiotic resistant E. coli strains. *Curr Nanosci*, 2015, 11(4): 527-538.

[9] V.S. Kotakadi, S.A. Gaddam, K. SucharithaVenkata, et al., New generation of bactericidal silver NPs against different antibiotic resistant *Escherichia coli* strains. *Appl Nanosci*, 2015, 5(7):847-855.

[10] V.S. Kotakadi, S.A. Gaddam, K. SucharithaVenkata, et al., Biofabrication and spectral characterization of silver NPs and their cytotoxic studies on human CD34 +ve stem cells. *3 Biotech*, 2016, 6(2): 216.

[11] S.A. Gaddam, V.S. Kotakadi, D.V.R.S. Gopal, et al., Efficient and robust biofabrication of silver NPs by *Cassia alata* leaf extract and their antimicrobial activity. *J Nanostruc Chem*, 2014, 4: 82.

[12] K. Khanra, S. Panja, I. Choudhuri, et al., Bactericidal and cytotoxic properties of silver NP synthesized from root extract of Asparagus racemosus. *Nano Biomed. Eng*, 2016, 8(1): 39-46.

[13] R. Subbiah, K. Muthuchelian, Development of nanodrug for treatment of breast cancer using Mallotus tetracoccus leaves - standardisation, synthesis and characterisation. *Nano Biomed. Eng*, 2016, 8(2): 82-90.

[14] M. Herlekar, S. Barve, and R. Kumar, Plant-mediated green synthesis of iron NPs. *J of NPs*, 2014, 2014: 140614.

[15] A. Tripathy, A.M. Raichur, N. Chandrasekaran, et al., Process variables in biomimetic synthesis of silver NPs by aqueous extract of *Azadirachtaindica* (Neem) leaves. *J Nanopart Res*, 2010, 12: 237-246.

[16] P.G. Mahlberg, Laticifers: An historical perspective. *The Botanical Review*, 1993, 59(1): 1-23.

[17] V.A. Litvin, R.L. Galagan, and B.F. Minaev. Kinetic and mechanism formation of silver NPs coated by synthetic humic substances. *Colloids and Surf A: Physicochemical and Eng Aspects*, 2012, 414: 234-243.

[18] D. de F Navarro Schmidt , R.A. Yunes, E.H. Schaab, et al., Evaluation of the anti-proliferative effect the extracts of Allamanda blanchetti and A. schottii on the growth of leukemic and endothelial cells. *J Pharm Pharm Sci*, 2006, 9(2): 200-208.

[19] A.S. Davis, A.J. Viera, and M.D. Mead, Leukemia: An overview for primary care. *Am Fam Physician*, 2014, *89*(9): 731-738.

[20] H. Bar, D.K. Bhui, G.P. Sahoo, et al., Green synthesis of silver NPs using latex of Jatropha curcas. *Colloids and Surf. A: Physicochem Eng Asp*, 2009, 339(1-3): 134-139.

[21] P. Banerjee, M. Satapathy, A. Mukhopahayay, et al., Leaf extract mediated green synthesis of silver NPs from widely available Indian plants: Synthesis, characterization, antimicrobial property and toxicity analysis. *Bioresources and Bioprocessing*, 2014, 1: 3.

[22] C. Robert, X. Lu, A. Law, et al., Macrophages.com: An on-line community resource for innate immunity research. *Immunobiology*, 2011, 216(11): 1203-1211.

[23] W. Strober, Trypan blue exclusion test of cell viability. *Curr Protoc Immunol*, 2001, Appendix 3: Appendix 3B.

[24] R. Pattern, A. Hirzel, Apoptosis DNA fragmentation analysis protocol. *Abcam*, 2017.

[25] M. Linga Rao, G. Bhumi, and N. Savithramma, Green synthesis of silver NPs by Allamandacathartica L. leaf extract and evaluation for antimicrobial activity. *Int J of Pharm Sci and Nanotech*, 2013, 6(4): 1-9.

[26] V.S. Kotakadi, S.A. Gaddam, Y. Subba Rao, et al., Biofabrication of silver NPs using Andrographis paniculata. *Eur J Med Chem*, 2014, 73: 135-140.

[27] V.A. Litvin, B.F. Minaev, Spectroscopy study of silver NPs fabrication using synthetic humic substances and their antimicrobial activity. *Spectrochimica Acta Part A: Molecular and Biomolecular Spectroscopy*, 2013, 108: 115-122.

[28] V.A. Litvin, B.F. Minaev, The size-controllable, one-step synthesis and characterization of gold NPs protected by synthetic humic substances. *Mater Chem Phys*, 2014, 144: 168-178.

[29] S. Chowdhury, A. Basu, and S. Kundu, Green synthesis of protein capped silver NPs from phytopathogenic fungus *Macrophomina phaseolina* (Tassi) Goid with antimicrobial properties against multidrug-resistant bacteria. *Nanoscale Res Lett*, 2014, 9: 1-11.

[30] A. Parveen, S. Rao, Cytotoxicity and genotoxicity of biosynthesized gold and silver NPs on Human cancer cell lines. *J of Cluster Sci*, 2014, 26(3): 775-788.

[31] P. Sanpui, P.A. Chattopadhyay, and S.S. Ghosh, Induction of apoptosis in cancer cells at low silver NP concentrations using chitosan nanocarrier. *ACS Appl Mater Interfaces*, 2011, 3(2): 218-228.

[32] J.L. Martindale, N.J. Holbrook, Cellular response to oxidative stress: signalling for suicide and survival. *J Cell Physiol*, 2002, 192(1): 1-15.